MOX-Report No. 23/2017

Computational models for hemodynamics

Quarteroni, A.; Vergara, C.

MOX, Dipartimento di Matematica
Politecnico di Milano, Via Bonardi 9 - 20133 Milano (Italy)

mox-dmat@polimi.it http://mox.polimi.it

Computational models for hemodynamics*

Alfio Quarteroni[1,2], Christian Vergara[2]

May 18, 2017

[1] Chair of Modelling and Scientific Computing, École Polytechnique Fédérale de Lausanne, Switzerland, alfio.quarteroni@epfl.ch
[2] MOX, Dipartimento di Matematica, Politecnico di Milano, Italy, {alfio.quarteroni,christian.vergara}@polimi.it

1 Synonyms

Mathematical modeling of the cardiovascular system.

2 Definitions

Mathematical foundation and numerical approximation of the cardiocirculatory system are addressed.

3 Background

Cardiovascular diseases represent the major cause of death in western countries, leading to more than 17.3 million deaths per year worldwide (about half of all deaths in Europe).

The cardiovascular system is composed by the *heart*, the *vascular circulation* (both arteries and veins), and the *microcirculation* (capillaries), see Figure 1. Here, the mathematical and numerical description of the first two components is considered.

The heart is composed by four chambers, two *atria* that collect blood coming from the vascular network, and two *ventricles* pumping blood into the vascular network. Atria and ventricles are connected by valves which open up when the atrial pressure is higher than the ventricular one allowing the blood to fill the

*This is an invited work by *Encyclopedia of Continuum Mechanics*

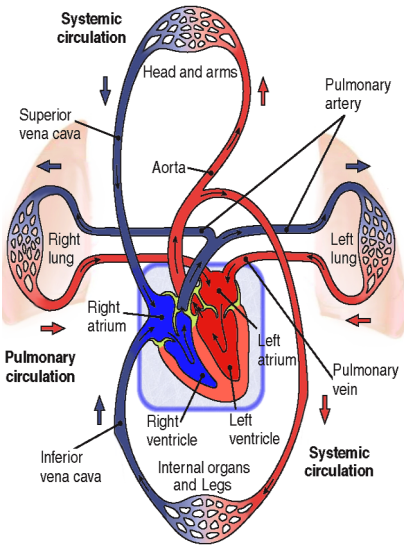

Figure 1: Representative scheme of the cardiovascular system.

ventricles, and close when blood starts flowing back to the atria. Valves govern as well the blood exchange between the ventricles and the vascular circulation. The heart wall is composed by the internal thin *endocardium*, the thick *myocardium* composed by fibers, and the external thin *epicardium*.

The pumping of blood into the vascular circulation is made possible by the heart contraction which is triggered by the propagation of an electrical signal (*action potential*), generating at the sino-atrial node in the right atrium, propagating through the atria and the *Purkinje network*, and finally spreading in all the ventricles myocardium. Electric propagation is due to the excitability of the heart cells, which produce a variation in membrane voltage when stimulated. The stimulation of an individual cell produces an action potential and the corresponding current allows for the excitation of the neighbour cells, and thus of the whole myocardium. The excitation of a heart cell corresponds to migration of ions through the cell membrane. In particular, there is an inward flux of extra-cellular calcium ions which allows for their binding with specific substances in the cell producing the contraction of the cell itself and of all the myocardium in a coordinated way.

The vascular circulation is composed by the *arteries* that bring the blood from the heart to the lungs and the microcirculation, and by the *veins* that allow the blood to return to the heart. Two circulations can be identified: the *systemic* circulation (left ventricle $\rightarrow$ systemic arteries $\rightarrow$ capillaries $\rightarrow$ systemic veins $\rightarrow$ right atrium), and the *pulmonary* circulation (right ventricle $\rightarrow$ pulmonary arteries $\rightarrow$ lungs $\rightarrow$ pulmonary veins $\rightarrow$ left atrium).

Blood is composed mainly of water and blood cells (red, white, and platelets). The diameter of blood cells is approximately $10^{-3}\,cm$, whereas that of the small-

est arteries and veins is about $10^{-1}\,cm$. Thanks to heart contraction, blood is pumped into the vascular circulation by means of discrete pulses with a pressure in the ranges $70-130\,mmHg$ and $20-30\,mmHg$ for the systemic and pulmonary arterial networks, respectively, and equal to about $10\,mmHg$ in the veins due to the high resistance in the microvasculature. Blood Reynolds number in arteries ranges from about 400 (in coronaries) to about 4000 (in the ascending aorta). In any case, the pulsatile nature of blood flow prevents full transition to turbulence to develop.

Blood flows in compliant vessels allow the proximal arteries to store a great amount of blood during the systole (the peak of the heart pulsatility) and the veins to act as reservoirs. This yields the propagation of a pressure wave along the arterial network. Vessel wall displacements are quite large, reaching up to 10% of their diameter. The vessel walls are mainly elastic; they are made of *elastin*, which is responsible for the linear behavior at small displacements, and by *collagen* which forms stiff fibres that induce a non-linear response at large strains.

4 The vascular circulation

4.1 Mathematical modeling

As stated above, blood flows in compliant vessels. From a mathematical point of view, this process can be described as a *fluid-structure interaction* (FSI) problem.

For the fluid (blood), well accepted hypotheses are incompressibility and homogeneity. Its rheology could be considered Newtonian for medium and large vessels [32] or non-Newtonian for small vessels such as coronaries or in presence of stenosis [40].

The deformation of the vessel wall is mathematically described by the elastodynamics equation. It is often assumed that a non-linear finite elastic law relates the stress tensor to the strain, and a nearly incompressible behavior [23]. To account for the preferred direction of the collagen fibres, anisotropic laws are usually considered. Unlike the fluid problem which is usually written in an Eulerian framework, the vessel wall problem is generally written in a Lagrangian configuration. To do so, given a function g defined in the current solid configuration Ω^t, we denote by $\widehat{g} = g \circ \mathcal{L}$ the same function in the reference configuration Ω, with $\mathcal{L}$ denoting the Lagrangian map. $\mathbf{F} = \nabla \mathbf{x}$ is the deformation tensor, $\mathbf{x}$ are the coordinates in the current configuration, $J = \det(\mathbf{F})$ represents the change of volume between the reference and the current configuration. The stress tensor in the reference configuration (*First Piola-Kirchhoff* stress tensor) is mapped into the current configuration (*Cauchy* stress tensor), as follows: $\widehat{\mathbf{T}}_s = J\mathbf{T}_s\mathbf{F}^{-T}$.

Figure 2 illustrates a representative situation with fluid and structure domains, whose common boundary is the fluid-solid (FS) interface Σ^t: it coincides with the physical fluid boundary and the internal vessel wall boundary. The

mathematical coupled problem at each time reads as follows:

$$\rho_f \left(\frac{\partial \mathbf{v}}{\partial t} + (\mathbf{v} \cdot \nabla)\mathbf{v} \right) - \nabla \cdot \mathbf{T}_f(\mathbf{v}, p) = \mathbf{0} \qquad \text{in } \Omega_f^t, \qquad (1a)$$

$$\nabla \cdot \mathbf{v} = 0 \qquad \text{in } \Omega_f^t, \qquad (1b)$$

$$\mathbf{v} = \frac{\partial \mathbf{d}}{\partial t} \qquad \text{at } \Sigma^t, \qquad (1c)$$

$$\mathbf{T}_s(\mathbf{d})\,\mathbf{n} = \mathbf{T}_f(\mathbf{v}, p)\,\mathbf{n} \qquad \text{at } \Sigma^t, \qquad (1d)$$

$$\rho_s \frac{\partial^2 \widehat{\mathbf{d}}}{\partial t^2} - \nabla \cdot \widehat{\mathbf{T}}_s(\widehat{\mathbf{d}}) = \mathbf{0} \qquad \text{in } \Omega_s, \qquad (1e)$$

$$\mathbf{d}_f = \mathbf{d} \qquad \text{at } \Sigma^t, \qquad (1f)$$

where $\mathbf{v}$ is the blood velocity, p the blood pressure, $\mathbf{T}_f$ the (Newtonian or non-Newtonian) Cauchy fluid stress tensor, $\mathbf{d}$ the vessel wall displacement, and $\mathbf{d}_f$ the fluid domain displacement; ρ_f and ρ_s denote the fluid and vessel wall densities.

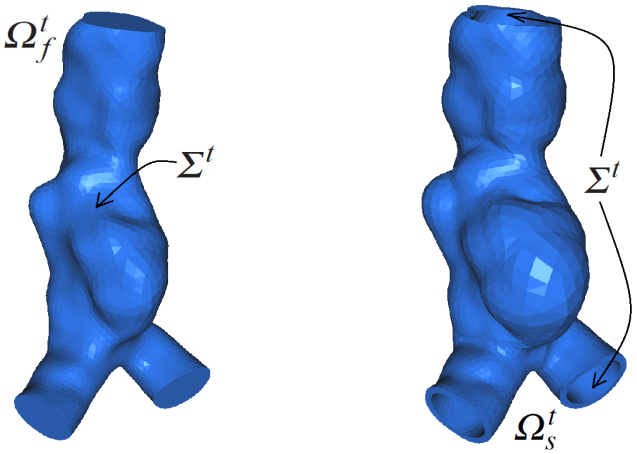

Figure 2: Representation of the fluid domain on the left and structure domain on the right. The bulge represents an abdominal aortic aneurysm.

In the coupled problem above, together with the Navier-Stokes equations (1a)-(1b) and the elasto-dynamics equation (1e), three interface coupling conditions are identified: the *kinematic* condition (1c) stating a no-slip assumption between fluid and structure particles; the *dynamic* condition (1d) expressing the action-reaction principle (III Newton law); and the *geometric* condition (1f) enforcing the perfect adherence between fluid and structure domains.

Problem (1) should be completed with suitable initial condition for $\mathbf{v}$, $\mathbf{d}$ and $\dot{\mathbf{d}}$, and boundary conditions. For the structure, the latter typically prescribe at the artificial sections homogeneous Dirichlet and Neumann conditions in the normal and tangential directions, respectively, and a Robin condition to account

for the presence of the surrounding tissue at the external surface. For the fluid problem, classical choices prescribe for example a Dirichlet condition for the blood velocity at the inlet and an absorbing Neumann or resistance condition at the outlet [30]. These values could be obtained either by means of clinical measures or by coupling the 3D model with reduced ones (1D or 0D), obtaining the so called *geometric multiscale* approach [39]. In both cases, the 3D problem is often supplemented with *defective* conditions which prescribe only average in space velocity or pressure data. Suitable numerical treatments are in this case mandatory to solve a well-posed problem [39].

4.2 Numerical approximation

For the numerical solution of the FSI problem (1), segregated algorithms are often considered, where the solution of the fluid and structure problems are solved separately in an iterative way. This allows to use pre-existing solvers to solve the coupled non-standard problem.

After time discretization (e.g. BDF2 or Crank-Nicolson for the fluid and Newmark for the structure), the fluid problem is linearized by means of a semi-implicit approach, where the convective term is extrapolated from previous time steps. This choice introduces a (mild) CFL-like restriction on the time step Δt to preserve absolute stability. We indicate with * extrapolated quantities. Given $\sigma_f \neq \sigma_s$, a general segregated algorithm reads as follows:

For $n \geq 1$, $k \geq 1$, at time step t^n/iteration k, until convergence or $k = k_{max}$,

1. solve the Oseen problem with a Robin condition at the FS interface:

$$\frac{\rho_f \alpha}{\Delta t}\mathbf{v}^n_{(k)} + \rho_f((\mathbf{v}^* - \mathbf{v}^*_f)\cdot\nabla)\mathbf{v}^n_{(k)} - \nabla\cdot\mathbf{T}_f(\mathbf{v}^n_{(k)}, p^n_{(k)}) = \mathbf{g}^n_f \qquad \text{in } \Omega^*_f, \tag{2a}$$

$$\nabla\cdot\mathbf{v}^n_{(k)} = 0 \qquad \text{in } \Omega^*_f, \tag{2b}$$

$$\sigma_f\mathbf{v}^n_{(k)} + \mathbf{T}_f\left(\mathbf{v}^n_{(k)}, p^n_{(k)}\right)\mathbf{n}^* = \sigma_f\left(\frac{\alpha}{\Delta t}\mathbf{d}^n_{(k-1)} + \mathbf{g}^n_{fs}\right) + \mathbf{T}_s\left(\mathbf{d}^n_{(k-1)}\right)\mathbf{n}^* \qquad \text{on } \Sigma^*; \tag{2c}$$

2. then, solve the non-linear vessel wall problem with another Robin condition at the FS interface:

$$\frac{\rho_s \beta}{\Delta t^2}\widehat{\mathbf{d}}^n_{(k)} - \nabla\cdot\widehat{\mathbf{T}}_s\left(\widehat{\mathbf{d}}^n_{(k)}\right) = \widehat{\mathbf{g}}^n_s \qquad \text{in } \Omega_s, \tag{3a}$$

$$\frac{\sigma_s \alpha}{\Delta t}\widehat{\mathbf{d}}^n_{(k)} + \widehat{\mathbf{T}}_s\left(\widehat{\mathbf{d}}^n_{(k)}\right)\widehat{\mathbf{n}} = \sigma_s\widehat{\mathbf{v}}^n_{(k)} + \widehat{\mathbf{T}}_f\left(\widehat{\mathbf{v}}^n_{(k)}, \widehat{p}^n_{(k)}\right)\widehat{\mathbf{n}} - \sigma_s\widehat{\mathbf{g}}^n_{fs} \qquad \text{on } \Sigma, \tag{3b}$$

where α and β are coefficients of the time discretization and the terms $\mathbf{g}$ account for the quantities at previous time steps.

Due to the fact that $\rho_f \simeq \rho_s$, in hemodynamics the choice $\sigma_f \to \infty$, $\sigma_s = 0$ and $k_{max} = 1$, i.e. the classical explicit *Dirichlet-Neumann* (DN) scheme used e.g. in aerodynamics, is unconditionally absolute unstable (high *added mass effect*, [6]). To obtain stable results in general, at least an implicit coupling between the fluid pressure and the vessel wall displacement is mandatory [12]. More in general, implicit algorithms should be considered, where iterations are solved until fulfillment of the interface conditions [38]. The convergence of the DN scheme requires a very small relaxation parameter and thus it is very slow [6]. To improve the convergence, suitable choices of the interface parameters σ_f and σ_s could be considered, see e.g. [2, 46].

In any case, at each iteration the fluid problem is solved in a (known) moving domain Ω_f^*. This corresponds to an explicit treatment of the geometric interface condition (1f). This choice produces stable results in hemodynamics, due to the restrained wall displacements [12]. For its solution, the fluid problem is often written in the *Arbitrary Lagrangian-Eulerian* configuration, i.e. in a framework moving with the fluid domain [20]. For the reconstruction of the latter, an harmonic extension of the geometric interface condition is usually adopted. The corresponding fluid linear system arising, e.g., after a Finite Elements discretization could be numerically solved e.g. with *projection* methods [7, 43] or block-preconditioned GMRES iterations [10].

On the other side, the vessel wall problem is linearized by means of the Newton method and the corresponding linear system arising at each iteration of the segregated algorithm could be solved e.g. by the coniugate gradient method preconditioned with FETI methods [3].

Instead of segregated algorithms, a different numerical approach to solve the FSI problem (1) is a *monolithic* approach, where an exact or inexact Newton method is applied to the whole non-linear FSI problem. The corresponding full linear system is solved by means of GMRES iterations preconditioned e.g. with additive Schwarz methods [4], global algebraic multigrid strategies [16], or block preconditioners [19, 9].

5 The heart

5.1 Mathematical modeling

From the modeling point of view, the heart function is the result of the interaction between blood flow inside the heart chambers and the electro-mechanical activity occurring in the myocardium. Mathematically, this is an FSI problem similar to that presented in the previous section, with FS interface being by the endocardium. However, a major difference is that unlike the vascular case where the vessel wall is completely passive and its deformation is determined only by the interaction with blood, here the structure problem has an active component

which produces the contraction. The forces generating this active component of the displacements are provided by the electrical propagation of the action potential.

Referring to Figure 3, left, the coupled problem occurring in the heart can be formally written as in (1), where the FS interface is now $\Sigma = \Sigma_{endo}$ and the structure problem (1e) is replaced by the following electro-mechanical problem:

$$\rho_s \frac{\partial^2 \widehat{\mathbf{d}}}{\partial t^2} - \nabla \cdot \left(\widehat{\mathbf{T}}_s^P(\widehat{\mathbf{d}}) + \widehat{\mathbf{T}}_s^A \left(\widehat{\mathbf{c}}, \widehat{\mathbf{d}}, \frac{d\widehat{\mathbf{d}}}{dt} \right) \right) = \mathbf{0} \qquad \text{in } \Omega_s, \quad (4a)$$

$$\widehat{\mathbf{T}}_s^A = P^A \mathbf{a}_f \otimes \widehat{\mathbf{a}}_f, \qquad P^A = \mathcal{A} \left(\widehat{\mathbf{c}}, \widehat{\mathbf{d}}, \frac{d\widehat{\mathbf{d}}}{dt} \right) \qquad \text{in } \Omega_s, \quad (4b)$$

$$C_m \frac{\partial V_m}{\partial t} - \nabla \cdot (\Sigma \nabla V_m) + I_{ion}\left(V_m, \mathbf{w}, \mathbf{c}\right) + I_{SAC}\left(V_m, \mathbf{d}\right) = I^{ext} \qquad \text{in } \Omega_s^t, \quad (4c)$$

$$\frac{\partial \mathbf{w}}{\partial t} = \mathbf{g}_w(V_m, \mathbf{w}) \qquad \frac{\partial \mathbf{c}}{\partial t} = \mathbf{g}_c(V_m, \mathbf{w}, \mathbf{c}) \qquad \text{in } \Omega_s^t. \quad (4d)$$

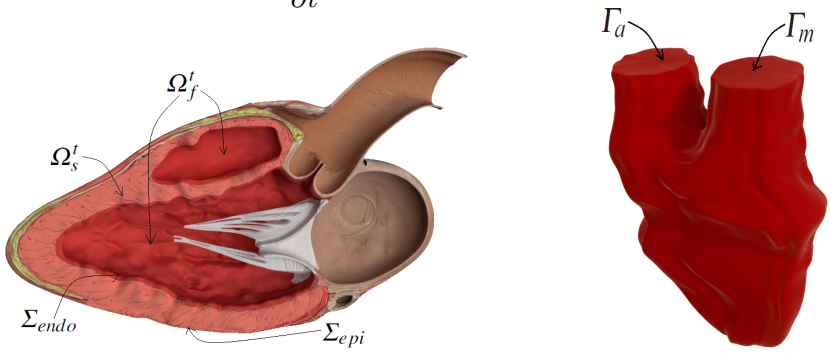

Figure 3: Left: longitudinal section of a complete heart domain. Right: fluid cavity in the left ventricle.

In this problem, (4a) represents the equation of elasto-dynamics for the myocardium, where $\mathbf{T}_s^P$ is the passive component of the stress tensor given by a non-linear elastic law similar to that of arteries where however two preferential directions (fibers and sheets) are often considered [22], and $\mathbf{T}_s^A$ is the active component of the stress regulated by the opening of calcium channels as a response to the depolarization. Equations (4b) used the most classical form of the active component, which acts in the fibers direction $\mathbf{a}_f$ and whose intensity P^A depends, through ordinary differential problems represented here by $\mathcal{A}$, on the ion (in particular calcium) concentration $\mathbf{c}$, the displacement $\mathbf{d}$, and the deformation rate $\dot{\mathbf{d}}$ [26, 27, 17]. Equation (4c) is the classical *monodomain* problem to describe the evolution of the transmembrane potential V_m, where C_m is the membrane capacitance multiplied by the surface area-to-volume ratio, Σ the conductivity tensor, I^{ext} and external applied current; I_{ion} are the *ionic currents* whose expression is suitably modeled by means of *reduced models* that provide

a description of the action potential and disregard sub-cellular processes [13], or *first* and *second generation models* that allow explicit description of the kinetics of different ionic currents [21]; I_{SAC} is the current activated by the deformation and provides a mechano-electrical feedback [28]. Finally, the monodomain problem is coupled with the systems of ordinary differential problems (4d), representing the cardiac cells model in the *gating* variables $\mathbf{w}$, i.e. the percentage of open channels per unit area of the membrane, and ion concentration variables $\mathbf{c}$. A more sophisticated model alternative to the monodomain one which allows a better description of pathological scenarios, is the *bidomain* model, see e.g. [8].

The coupled electro-mechanical-fluidic problem (1a)-(1b)-(1c)-(1d)-(4)-(1f) should be completed with suitable initial conditions for $V_m, \mathbf{w}, \mathbf{c}, \mathbf{v}$, $\mathbf{d}$ and $\dot{\mathbf{d}}$, and boundary conditions. For the electrical problem, the latter usually prescribe homogeneous Neumann conditions at Σ_{epi} and Σ_{endo}, whereas for the mechanics a Robin condition similar to the vascular case is prescribed at Σ_{epi}, even if more sophisticated models of interaction with the pericardium have been also proposed [15]. Moreover, for the electrical problem, forcing terms in correspondence of the junctions connecting the myocardium to the Purkinje network should be considered to account for the propagation in such a network [45, 44]. For the fluid problem, boundary interfaces are provided by the valves (except from the interface between atria and vascular circulation), see Figure 3, right, where the case of the left ventricle is depicted, Γ_m and Γ_a being the interfaces with the left atrium (mitral valve) and arterial circulation (aortic valve). In this case, another FSI problem should be considered between blood and valve leaflets [33, 5, 18]. However, often simplified valve models have been considered in order to reduce the complexity of the problem, see e.g. [25, 1, 11].

5.2 Numerical approximation

For the numerical discretization of the electrical problem (4c)-(4d), a special care should be taken in the choice of time and space discretization parameters, which should be fine enough to capture the very steep and fast propagating electrical front. Classical numerical strategies include *semi-implicit* methods where the transmembrane potential V_m is treated explicitly both in the ODE systems (4d) and in the ionic term I_{ion} [24], and *operator splitting-based methods* that separate the reaction operator from the diffusive one [35].

For the electro-mechanical coupled problem (4), a possible splitting strategy consists in solving first the electrical problem (4c)-(4d) with an explicit treatment of the displacements, then update the active stress contribution (4b), and finally solve the mechanics (4a) by means of Newton iterations [26]. An alternative, more stable, scheme is obtained by updating the active stress contribution at each Newton iteration [29]. A different scheme has been proposed in [31], where the ODE systems (4d) are solved first, then Newton iterations are applied to the mechanical problem (4a)-(4b), and finally the electrical problem (4c) is solved.

Once the solution of the electro-mechanical problem is obtained, it could be

coupled by means of segregated schemes with the fluid solution in order to obtain a numerical solution of the whole coupled electro-mechanical-fluidic problem (1a)-(1b)-(1c)-(1d)-(4)-(1f). Alternative strategies are obtained by considering block-preconditioned monolithic solvers for the solution of the whole coupled problem [36].

6 Conclusions

Several books, monographs and review papers have been published in recent years for the mathematical description of the cardiovascular system, see e.g. [34, 41, 14, 42, 8, 37], highlighting the great interest of the mathematical, engineering, and clinical communities on this topic. However, many important related fields are still far from being throughly investigated and/or have not still been coupled with the cardiovascular system. This is the case e.g. of the *venous system*, *metabolic system*, *respiratory system*, *cerebro-spinal fluid circulation*, *nervous system*, and *limphatyc system*. This opens new and attractive challenges for future development of mathematical and computational methods to have a complete representation of the cardiovascular system.

References

[1] M. Astorino, J. Hamers, C.S. Shadden, and J.F. Gerbeau. A robust and efficient valve model based on resistive immersed surfaces. *International Journal for Numerical Methods in Biomedical Engineering*, 28(9):937959, 2012.

[2] S. Badia, F. Nobile, and C. Vergara. Fluid-structure partitioned procedures based on Robin transmission conditions. *J. Comput. Phys.*, 227:7027–7051, 2008.

[3] D. Balzani, D. Brands, A. Klawonn, O. Rheinbach, and J. Schroder. On the mechanical modeling of anisotropic biological soft tissue and iterative parallel solution strategies. *Archive of Applied Mechanics*, 80(5):479–488, 2010.

[4] A. Barker and X.C. Cai. Scalable parallel methods for monolithic coupling in fluid-structure interaction with application to blood flow modeling. *J. Comput. Phys.*, 229:642–659, 2010.

[5] D. Boffi and L. Gastaldi. A finite element approach for the immersed boundary method. *Comp. and Struct*, 81(8-11):491–501, 2003.

[6] P. Causin, J.F. Gerbeau, and F. Nobile. Added-mass effect in the design of partitioned algorithms for fluid-structure problems. *Comput. Methods Appl. Mech. Engrg.*, 194(42-44):4506–4527, 2005.

[7] A.J. Chorin. Numerical solution of the Navier–Stokes equations. *Mathematics of Computation*, 22:745–762, 1968.

[8] P. Colli Franzone, L.F. Pavarino, and S. Scacchi. *Mathematical Cardiac Electrophysiology*. Springer, 2014.

[9] P. Crosetto, S. Deparis, G. Fourestey, and A. Quarteroni. Parallel algorithms for fluid-structure interaction problems in haemodynamics. *SIAM J. Sci. Comput.*, 33:1598–1622, 2011.

[10] H. Elman, D. Silvester, and A. Wathen. *Finite Elements and Fast Iterative Solvers*. Oxford Science Publications, 2005.

[11] M. Fedele, E. Faggiano, L Dedè, and A. Quarteroni. A patient-specific aortic valve model based on moving resistive immersed implicit surfaces. MOX-Report n. 23-2016, Department of Mathematics, Politecnico di Milano, Italy, 2016.

[12] M.A. Fernández, J.F. Gerbeau, and C. Grandmont. A projection semi-implicit scheme for the coupling of an elastic structure with an incompressible fluid. *Int. J. Numer. Meth. Engrg.*, 69(4):794–821, 2007.

[13] R. FitzHugh. Impulses and physiological states in theoretical models of nerve membrane. *Biophys J*, 1(6):445–466, 1961.

[14] L. Formaggia, A. Quarteroni, and A. Veneziani (Eds.). *Cardiovascular Mathematics - Modeling and simulation of the circulatory system*. Springer-Verlag Milan, 2009.

[15] T. Fritz, C. Wieners, G. Seemann, H. Steen, and O. Dossel. Simulation of the contraction of the ventricles in a human heart model including atria and pericardium. *Biomechanics and Modeling in Mechanobiology*, 13(3):627–641, 2014.

[16] M.W. Gee, U. Kuttler, and W.A. Wall. Truly monolithic algebraic multigrid for fluid-structure interaction. *Int. J. Numer. Meth. Engrg.*, 85(8):987–1016, 2011.

[17] S. Goktepe and E. Kuhl. Electromechanics of the heart: a unified approach to the strongly coupled excitationcontraction problem. *Computational Mechanics*, 45(2):227–243, 2010.

[18] J. De Hart, G.W.M. Peters, P.J.G. Schreurs, and F.P.T. Baaijens. A two-dimensional fluidstructure interaction model of the aortic value. *Journal of biomechanics*, 33(9):10791088, 2000.

[19] M. Heil. An efficient solver for the fully coupled solution of large-displacement fluid-structure interaction problems. *Comput. Methods Appl. Mech. Engrg.*, 193:1–23, 2004.

[20] C.W. Hirt, A.A. Amsden, and J.L. Cook. An arbitrary lagrangian eulerian computing method for all flow speeds. *J. Comput. Phys.*, 69:277–324, 1974.

[21] A.L. Hodgkin and A.F. Hukley. A quantitative description of membrane current and its application to conduction and excitation in nerve. *J Physiol*, 117(4):500–544, 1952.

[22] G.A. Holzapfel and R.W. Ogden. Constitutive modelling of passive myocardium: a structurally based framework for material characterization. *PHILOSOPHICAL TRANSACTIONS of the Royal society A*, 367:3445–3475, 2009.

[23] G.A. Holzapfel and R.W. Ogden. Constitutive modelling of arteries. *Proc. R. Soc. Lond. Ser. A Math. Phys. Eng. Sci.*, 466(2118):1551–1596, 2010.

[24] J.P. Keener and K. Bogar. A numerical method for the solution of the bidomain equations in cardiac tissue. *Chaos*, 8:234–241, 1998.

[25] T. Korakianitis and Y. Shi. A concentrated parameter model for the human cardiovascular system including heart valve dynamics and atrioventricular interaction. *Medical Engineering & Physics*, 28(7):613–628, 2006.

[26] M.P. Nash and A.V. Panfilov. Electromechanical model of excitable tissue to study reentrant cardiac arrhythmias. *Progress in Biophysics and Molecular Biology*, 2-3(85):501–522, 2004.

[27] S.A. Niederer, P.J. Hunter, and N.P. Smith. A quantitative analysis of cardiac myocyte relaxation: A simulation study. *Biophysical Journal*, 90(5):1697–1722, 2006.

[28] S.A. Niederer and N.P Smith. A mathematical model of the slow force response to stretch in rat ventricular myocytes. *Biophysical Journal*, 92(11):4030–4044, 2007.

[29] S.A. Niederer and N.P Smith. An improved numerical method for strong coupling of excitation and contraction models in the heart. *Progress in Biophysics and Molecular Biology*, 96(1–3):90–111, 2008.

[30] F. Nobile and C. Vergara. An effective fluid-structure interaction formulation for vascular dynamics by generalized Robin conditions. *SIAM J Sc Comp*, 30(2):731–763, 2008.

[31] L.F. Pavarino, S. Scacchi, and S. Zampini. Newton–krylov-bddc solvers for nonlinear cardiac mechanics. *Computer Methods in Applied Mechanics and Engineering*, 295:562–580, 2015.

[32] K. Perktold, E. Thurner, and T. Kenner. Flow and stress characteristics in rigid walled and compliant carotid artery bifurcation models. *Medical and Biological Engineering and Computing*, 32(1):19–26, 1994.

[33] C. Peskin. Flow patterns around heart valves: A numerical method. *J. Comput. Phys.*, 10(2):252–271, 1972.

[34] C. Peskin. The immersed boundary method. *Acta Numerica*, 11:479–517, 2002.

[35] Z. Qu and A. Garfinkel. An advanced algorithm for solving partial differential equation in cardiac conduction. *IEEE Transaction on Biomedical Engineering*, 46(9):1166–1168, 1998.

[36] A. Quarteroni, T. Lassila, S. Rossi, and R. Ruiz-Baier. Integrated heart - coupling multiscale and multiphysics models for the simulation of the cardiac function. *Comput. Methods Appl. Mech. Eng.*, 314:345–407, 2017.

[37] A. Quarteroni, A. Manzoni, and C. Vergara. The cardiovascular system: Mathematical modelling, numerical algorithms and clinical applications. *Acta Numerica*, 26:365–590, 2017.

[38] A. Quarteroni and A. Valli. *Domain Decomposition Methods for Partial Differential Equations*. Oxford Science Publications, 1999.

[39] A. Quarteroni, A. Veneziani, and C. Vergara. Geometric multiscale modeling of the cardiovascular system, between theory and practice. *Comput. Methods Appl. Mech. Engrg.*, 302:193–252, 2016.

[40] A.M. Robertson, A. Sequeira, and R.G. Owens. Rheological models for blood. In *Cardiovascular mathematics, edited by L. Formaggia, A. Quarteroni, A. Veneziani, Chapter 6*, pages 211–241. Springer, 2009.

[41] N. P. Smith, D. P. Nickerson, E. J. Crampin, and P. J. Hunter. Multiscale computational modelling of the heart. *Acta Numerica*, 13:371–431, 2004.

[42] C.A. Taylor and C.A. Figueroa. Patient-specific modeling of cardiovascular mechanics. *Annual Review of Biomedical Engineering*, 11:109–134, 2009.

[43] R. Temam. Sur l'approximation de la solution des équations de Navier–Stokes par la méthode des pas fractionaires (I). *Archives for Rational Mechanics and Analysis*, 32:135–153, 1969.

[44] C. Vergara, M. Lange, S. Palamara, T. Lassila, A.F. Frangi, and A. Quarteroni. A coupled 3D-1D numerical monodomain solver for cardiac electrical activation in the myocardium with detailed Purkinje network. *J. Comput. Phys*, 308:218–238, 2016.

[45] E.J. Vigmond and C. Clements. Construction of a computer model to investigate sawtooth effects in the Purkinje system. *IEEE Trans Biomed Eng*, 54(3):389–399, 2007.

[46] Y. Yu, H. Baek, and G.E. Karniadakis. Generalized fictitious methods for fluidstructure interactions: Analysis and simulations. *J. Comput. Phys.*, 245:317–346, 2013.

MOX Technical Reports, last issues

Dipartimento di Matematica
Politecnico di Milano, Via Bonardi 9 - 20133 Milano (Italy)

22/2017 Bartezzaghi, A.; Dede', L.; Quarteroni, A.
Biomembrane modeling with Isogeometric Analysis

21/2017 Talska, R.; Menafoglio, A.; Machalova, J.; Hron, K.; Fiserova, E.
Compositional regression with functional response

18/2017 Ambartsumyan, I.; Khattatov, E.; Yotov, I.; Zunino, P.
A Lagrange multiplier method for a Stokes-Biot fluid-poroelastic structure interaction model

19/2017 Giovanardi, B.; Formaggia, L.; Scotti, A.; Zunino P.
Unfitted FEM for modelling the interaction of multiple fractures in a poroelastic medium

20/2017 Albrecht G.; Caliò F.; Miglio E.
Fair surface reconstruction through rational triangular cubic Bézier patches

16/2017 Ghiglietti, A.; Scarale, M.G.; Miceli, R.; Ieva, F.; Mariani, L.; Gavazzi, C.; Paganoni, A.M.; E
Urn models for response-adaptive randomized designs: a simulation study based on a non-adaptive randomized trial

15/2017 Tagliabue, A; Dede', L.; Quarteroni A.
Complex blood flow patterns in an idealized left ventricle: a numerical study

14/2017 Bruggi, M.; Parolini, N.; Regazzoni, F.; Verani, M.
Finite Element approximation of an evolutionary Topology Optimization problem

13/2017 Gigante, G.; Vergara, C.
Optimized Schwarz Methods for circular flat interfaces and geometric heterogeneous coupled problems

17/2017 Agosti, A.
Error Analysis of a finite element approximation of a degenerate Cahn-Hilliard equation